

3D electrode architectures for high energy and high power lithium-ion batteries

W. Pflöging*

Karlsruhe Institute of Technology, IAM-AWP, P.O. Box 3640, 76021 Karlsruhe, Germany

ABSTRACT

There is worldwide a strong effort to increase energy and power density on battery level for future electric vehicles. In addition, the demand for cost efficient, reliable, and long lifetime lithium-ion batteries (LIB) is continuously increasing. For the development of next-generation LIB a new scientific-technical approach was established by merging the 3D battery concept with high mass-loaded electrodes. The 3D battery concept is realized by laser structuring of electrodes and has a huge impact on high rate capability and lifetime of lithium-ion batteries. In frame of process up-scaling, ultrafast laser ablation including roll-to-roll processing was established for thick film electrodes without damaging the active material. Post-mortem studies using laser-induced breakdown spectroscopy were carried out to study degradation processes and to illustrate the formation of new lithium diffusion pathways in 3D electrodes. The studies were performed with lithium nickel manganese cobalt oxide as cathode and graphite/silicon as anode. Silicon has the benefit to provide one order of magnitude higher gravimetric energy density than the common used graphite. However, a bottleneck of silicon is its huge volume change of 300 % during electrochemical cycling. High mechanical tension may arise, which results in crack formation, continuous formation of solid electrolyte interphase, and subsequent electrode delamination. It was shown that batteries with laser structured electrodes benefit from a homogenous lithiation and delithiation, reduced compressive stress, and overall improved electrochemical properties in comparison to batteries with unstructured electrodes. A new manufacturing tool is presented for next-generation battery production to overcome current limitations in electrode design and cell performance.

Keywords: lithium-ion battery, 3D battery, electrode manufacturing, laser structuring, silicon-based anode, lithium nickel manganese cobalt oxide, laser-induced breakdown spectroscopy, roll-to-roll processing

1. INTRODUCTION AND BACKGROUND

Lithium-ion batteries (LIBs) have become the most important energy storage device for electric vehicles (EVs) [1]. A decade ago, the production costs of LIBs, based on the kilowatt hour, were almost an order of magnitude higher than today's costs [2, 3]. For the year 2025, further cost reductions to well below USD 100 per kilowatt hour are expected [4]. A further increase in the performance and thus acceptance of EVs is closely linked to the further development of the LIBs. This is characterized by a further increase in the available power and energy density [5] and the rapid charging options for batteries. In order to significantly increase the range of EVs to more than 600 km, the energy densities on cell level must reach 350-500 Wh/kg in the future [6]. Batteries of "Generation 1" and "Generation 2a" are predominantly used in the electric vehicles available on the market today, see Figure 1 [7]. These are cells which on the cathode side are based on lithium iron phosphate (LFP) with an olivine structure, LiMn_2O_4 (LMO) spinels, or layered oxides such as lithium nickel cobalt aluminum oxide (NCA) or lithium nickel manganese cobalt oxide (NMC 111). On anode side these cells are based on natural or artificial graphite or amorphous carbon (Figure 1).

In order to be able to increase energy and power density at the same time, both a material development and a development of the electrode architecture are required. On the cathode side, nickel-rich NMC materials with a low cobalt content are increasingly being used with specific capacities in the range of up to 190 mAh/g [8]. By means of suitable doping measures and coating methods, the stability of these active materials has now been improved to such an extent that NMC 622 has already replaced NMC 111 as the state-of-the-art material [9]. It is foreseeable that this trend will continue in the future

* wilhelm.pfluegling@kit.edu; phone +49 721 608 22889; <http://www.iam.kit.edu/awp/165.php>

and that NMC 622 will be replaced by NMC 811 and also by cobalt-free materials such as LMNO (lithium nickel manganese oxide), which is also considered a high-voltage material [10]. In addition to the question of the suitable active material on the cathode side with sufficient specific capacity, cycle stability, and long-term stability, these materials should be compatible with the solvent water when processed in order to avoid the organic solvent NMP (N-methyl-2-pyrrolidone), which has been usually used up to now. NMP is harmful to health, represents a burden on the environment, and must therefore be recovered using cost-intensive processes during the electrode drying procedure [11]. The coating with aqueous cathode slurries and in particular for nickel-rich NMC is associated with an increase in the pH value, which leads to corrosion of the aluminum current collector and a degradation of active material during wet electrode coating [12, 13]. To avoid this, different process strategies and NMC material modifications have been investigated and developed [14]. Recently, Leclanché as a battery manufacturer report about successful use of water-based NMC 622 slurries in LIB development [15]. Promising research related to water-based NMC811 electrodes has recently been reported as well [16].

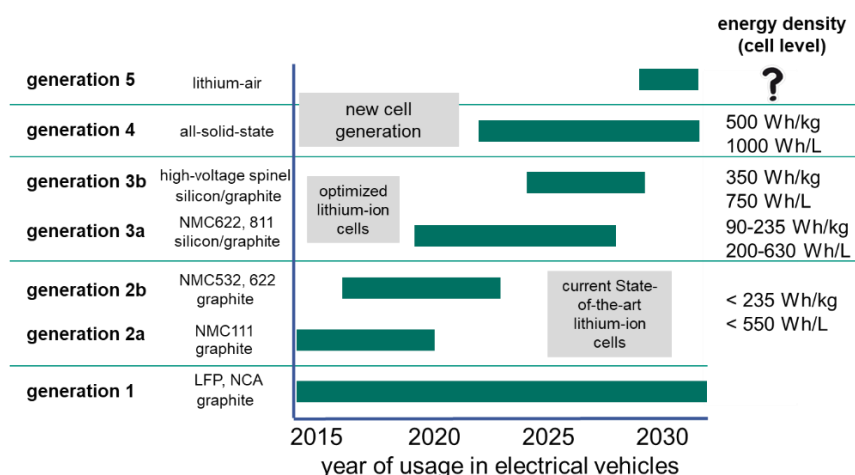


Figure 1: Overview of the different cell generations for electromobility. Values extracted from [7] and [17].

In addition to the material development, the electrode architecture has to be improved in order to achieve high energy densities at the cell level. The thick film concept is ideal for this. As already calculated in [17] for the NMC 111 system, increasing the layer thickness from 50 μm (state-of-the-art) to values in the range of 200 μm to 300 μm can contribute to an increase in energy density of more than 20-30% up to values of 250 Wh/kg and 580 Wh/L. The higher mass loading of the individual electrodes means that less inactive material, such as current collectors and separator materials, has to be used in the battery. This ultimately leads to an increase in the gravimetric and volumetric energy density. For NMC 811, which has a specific energy density that is approx. 30 % higher than that of NMC 111, energy densities can be further increased for the next generation of lithium-ion batteries. A value of 350 Wh/kg (at cell level) is given as target for next generation EV applications [18].

Despite this very plausible thick-layer concept, the following limitation must be noted: high layer thicknesses or mass loading lead to extended lithium transport pathways within the composite electrodes. This in turn causes an increasing diffusion overpotential, which is getting more pronounced at high battery power operation. This means that with increasing mass loading of the electrodes, the available capacity during discharging decreases sharply at high power levels. High energy densities and high power densities can therefore not easily be realized simultaneously. The term “C-rate” is used to describe the level of applied power densities. The C-rate indicates the current with which the battery is discharged or charged, based on the practical capacity of the cell. For example, at a C rate of 2C or 3C, the cell will be fully discharged or charged within 30 minutes or 20 minutes, respectively. With an increasing C-rate and layer thickness, the cell polarization increases until finally the capacity of the cell drops to zero. To overcome this bottleneck, the 3D battery concept was introduced to enable both high energy densities through the thick-film concept and high power densities at high C-rates [17, 19]. The 3D battery concept was initially developed for micro batteries and, through 3D structuring of the electrodes, increases the active surface and shortens the lithium-ion transport pathways [20]. This has a direct impact on the diffusion kinetics, the degradation processes (mechanical, chemical), and thus also on the electrochemical performance of the battery. For example, the high-current capability of the battery is improved and the impedance values are reduced. A main challenge was to transfer 3D battery concept to thick film composite electrodes. Different types of structures are possible such as hole, line, or grid patterns (Figure 2).

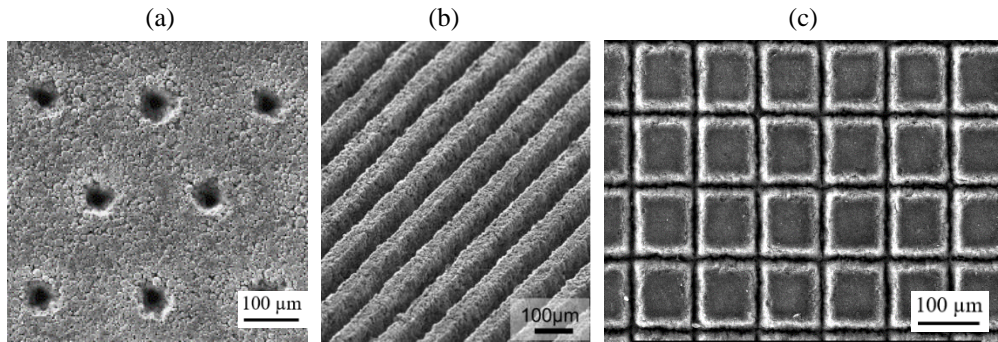


Figure 2: Scanning electron microscopy (SEM) images of (a) laser-generated hole (lithium nickel manganese cobalt oxide (NMC) electrode), (b) line (lithium iron phosphate (LFP) electrode), and (c) grid (silicon-graphite electrode) structures.

While thin film electrodes are useful for high power application, thick film electrodes are useful for high energy applications. The 3D battery concept now merges both approaches. For this purpose, structuring via ultrafast laser ablation was established as a suitable technology to draw 3D electrodes architectures. Upscaling the laser process is currently an important challenge to enable the integration of the technology into battery manufacturing. The adaptation of the laser process speed to the high coating speeds in the range of 30 m/min for state-of-the-art electrodes and the adaptation of the process control to ultra-thick electrodes with a layer thickness of up to 300 μm are essential development steps. On the anode side, there are similar challenges with regard to process upscaling as for the cathode. In recent technological approaches flanked by the industrial project called NextGen-3DBat, funded by the German Federal Ministry of Education and Research, KIT is transferring this technology in a pilot line by roll-to-roll processing using recently developed high repetition ultrashort pulse lasers with average laser powers up to 500 W [21]. The development of the next generation of anodes (“generation 3”) is being pursued in direction of silicon-graphite composite electrodes. Silicon (Si) enables specific capacities that are almost an order of magnitude higher than that of the commonly used graphite with maximum specific capacities of up to 372 mAh/g [22]. However, during battery operation, silicon undergoes a significant volume change of up to 300 %, which is a well-known issue in the current efforts of commercialization of silicon-based anodes. Cracks in active material particles occur with these enormous changes in volume and ultimately lead to pulverization of the material, disruption of the electrical conduction paths built up by conductive black, and also to film delamination [23]. It is therefore the subject of current research and development to significantly improve the mechanical integrity of silicon-based anodes in order to create the conditions for establishing silicon anodes in next-generation batteries. The key characteristics here are an improved cycle life, cycle stability, and capacity retention [24]. The use of silicon-graphite composite layers in combination with a 3D electrode architecture appears to be a very promising approach and its enabling further to introduce high mass loadings as well [25, 26].

Although graphite has a lower specific capacity, as an electrode scaffold it can enable improved volumetric energy density, cycle stability, and a long service life (> 1000 cycles), while silicon contributes significantly to increasing the specific capacity on the anode side [27, 28]. Similar to the cathode structuring described above, 3D architectures can be realized precisely by ultrafast laser structuring. This has been successfully implemented so far on a laboratory scale [25, 29]. By introducing free-standing electrode microstructures, e.g., so-called grid structures, mechanical compressive stresses within the silicon-graphite (Si/C) electrodes can be significantly reduced and an improvement in rate capability, cycle stability, and cell life can be achieved [25].

Lithium concentration profiles in laser-structured and unstructured electrodes as a function of the C rate in the lithiated and delithiated state provide valuable information about the diffusion kinetic influence of the 3D electrode architecture and are correlated with the electrochemical data, the cell performance, and the aging processes for further structure optimization. For this purpose, the laser-induced breakdown spectroscopy (LIBS) was successfully applied for anodes and cathodes [26, 30-33]. With LIBS, the binder distribution, which depends on the drying conditions, can also be determined over a large footprint area for ultra-thick film electrodes and used for further optimization of the electrode coating and subsequent drying process [17].

2. EXPERIMENTAL

2.1 Battery Materials

Commercially active materials were selected for electrode coating development via tape casting with a doctor blade (ZUA 2000.100, Proceq, Schwerzenbach, Switzerland) using a lab coater (MSK-AFA-L800-LD, MTI Corporation, Richmond, CA, USA). The thickness of the coated electrode layers was controlled by varying the gap of the doctor blade. On cathode side NMC 622 powder (BASF SE, Ludwigshafen, Germany) with a particle size of 12.8 μm (D90) was used while on anode side active materials were applied such as flake-like graphite (Targray, Technology International Inc., Kirkland, QC, Canada) with median diameter $D_{50} = 15.26 \mu\text{m}$ and nano-sized silicon particles with an average particle size of 150 nm (2W iTech, LLC, San Diego, CA, USA). For the electrode slurry preparation different types of binders were introduced such as NMP-based polyvinylidene fluoride (PVDF, MTI corporation, USA), water-based carboxymethyl cellulose (CMC, CRT 2000PA, DoeWolff Cellulosic, Bomlitz, Germany), styrene-butadiene rubber (SBR) (MTI Corporation, USA), and water-based fluorine acrylic copolymer latex TRD 202A (JSR Micro NV, Leuven, Belgium). Finally, carbon black C-ENERGY Super C65 (Imerys G & C Belgium, Willebroek, Belgium) or Timcal Super C65 (MTI Corporation, Richmond, CA, USA) were used as conductive additives. Detailed descriptions of the respective recipes for anodes and cathodes can be found in [25, 26, 30] and [14, 34, 35], respectively. The slurries were tape casted onto thin metallic aluminum (cathode) and copper (anode) current collector foils. Prior to laser structuring, the electrode was calendered using a hot rolling press machine (HR01 Hot Rolling Machine, MTI Corporation, Richmond, CA, USA). Finally, the prepared electrodes reveal a porosity of 35 % (cathode) or 42 % (anode).

2.2 Laser Structuring and Cutting on Roll-to-Roll Systems

Laser materials processing systems, PS450-TO (Optec s.a., Frameries, Belgium) and MSV-203 (M-Solv Ltd., Oxford, UK), were provided with different ultrafast laser sources providing medium laser average powers up to 35 W (Satsuma and Tangerine type, Amplitude Systèmes s.a., Bordeaux, France) and ultrafast laser systems with high average laser power of 300 W and 500 W (FX600 types, EdgeWave GmbH, Würselen, Germany). Both processing systems are each equipped with roll-to-roll systems and large field scanner systems in order to be able to process commercial and advanced electrode materials with a large footprint. The femtosecond lasers operate at a fundamental wavelength of 1030 nm or at its second harmonic (wavelength: 515 nm) with a pulse duration in the range of 280 fs ($f_s=10^{-15}$ s) to 10 ps ($p_s=10^{-12}$ s). Laser pulse repetition rates from 100 kHz up to 50 MHz can be applied for electrode cutting and structuring [21].

2.3 Battery Operation

Coin cells of type CR2032 (MTI Corporation, Richmond, CA, USA) and lab pouch cells (electrode footprint up to 80 x 80 mm²) were used to characterize the electrochemical properties of the laser-structured and unstructured electrodes. Cell assembly was performed in a glove box filled with argon (LABmaster SP, MBraun Inertgas-Systeme GmbH, Munich, Germany) in a high-purity atmosphere ($\text{O}_2 < 0.1$ ppm, $\text{H}_2\text{O} < 0.1$ ppm). Coin cell types consist of circular electrodes having a diameter of 12 mm and a counter electrode namely lithium metal foil (Sigma Aldrich, St. Louis, MO, USA) with a thickness of 250 μm and a diameter of 11 mm. The used separator material acting as electrical insulator between the electrodes were either glass fiber separators (GF/A filter, thickness 260 μm , Whatman, Maidstone, UK) or polypropylene (PP) sheets (Celgard, Charlotte, NC, USA) with a thickness of 25 μm . The used electrolyte consists of a 1.3 mol/L lithium hexafluorophosphate (LiPF_6) in ethylene carbonate (EC) and ethyl methyl carbonate (EMC) solution with a weight ratio of 3:7. Additionally, 5 wt% fluoroethylene carbonate (FEC) was added to the mixture, which can contribute to the formation of a more stable solid electrolyte interphase (SEI). The coin cell components were assembled using an electric coin cell crimper (MSK-160D, MTI Corporation, Richmond, CA, USA). The electrochemical measurements were performed at room temperature 22 °C applying devices from Arbin Instruments (BT 2000, College Station, TX, USA) or by BioLogic Science Instruments (VMP-3, Seyssinet-Pariset, France). More detailed information regarding formation and cycling procedures can be found in [14, 36].

2.4 Laser-Induced Breakdown Spectroscopy

Laser-induced breakdown spectroscopy (LIBS) was performed on electrodes subsequently to electrochemical analysis, starting from the top of the composite layer towards the current collector. For this purpose a laser-induced plasma was generated by a passive-mode-locked Nd:YAG laser (wavelength 1064 nm; pulse length 1.5 ns; pulse energy 3 mJ; laser repetition rate 100 Hz; focus diameter on sample 100 μm) which was integrated in an analytic chamber system from Secopta GmbH, Germany. The plasma light of each laser ablation pulse was analyzed by a Czerny-Turner spectrometer (type: FiberLIBS SN013, Secopta GmbH, Teltow, Germany). The detector covers spectral ranges of 229 - 498 nm and

569 - 792 nm. The data were analyzed by SEC Viewer 1.9 (Secopta GmbH, Teltow, Germany). The intensities of the respective specific emission wavelengths of each element enable, overall, a complete quantitative or qualitative stoichiometric analysis of the electrode. Due to the effect of self-absorption at the wavelength of 670.77 nm, the Li^{I} emission wavelength of 610.35 nm was used for the analysis of lithium [31]. The calibration data were derived from LIBS and inductively coupled plasma atomic emission spectroscopy (ICP-OES) as described in [31, 33]. Lithium concentration and distribution related to C-rates were systematically investigated in structured and unstructured electrodes [26, 30-33, 37].

3. RESULTS AND DISCUSSION

3.1 Cathode

The 3D battery concept improves the lithium-ion diffusion kinetics. However, one further important benefit of laser structuring of electrodes is its impact on electrode wetting with liquid electrolyte. While transferring the 3D battery concept into composite cathodes by forming line patterns it became quite obvious that those line patterns can act as capillary structures which turns electrodes into superwicking [38]. Laser generated micro-sized grooves act as capillary structures which soak the liquid electrolyte into the composite electrode. Each nano- and micro-sized pore is instantaneously filled with liquid electrolyte. The complete electrode is rapidly and homogeneously wetted within a few seconds while unstructured electrodes show no significant wetting behavior. In unstructured state-of-the-art electrodes, dry electrode areas can be remained which are starting points for cell degradation. The benefits of electrode capillary structures are quite evident. In state-of-the-art cell manufacturing the dry electrode stack undergoes a complex and time consuming electrolyte filling and vacuum processes and subsequent warm aging are necessary before electrochemical formation is performed [3]. By using laser structured electrodes, the repeated electrolyte filling and warm aging procedure can be avoided. After electrolyte filling the battery can be directly forwarded to electrochemical formation. It could be proven that without warm aging process, batteries with unstructured electrodes show a dramatical cell failure after a few hundred cycles while cells with structured electrodes show a quite stable capacity retention [38]. However, even the best produced batteries without structured electrodes but with warm aging show a decreased cell lifetime in comparison to pouch cells with structured electrodes, and a spontaneous cell failure after 1000 cycles (Figure 3).

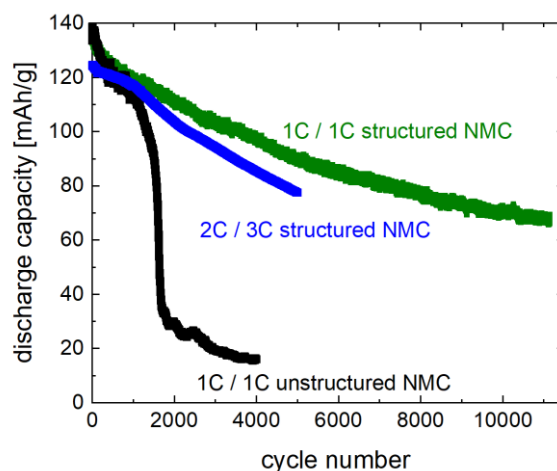


Figure 3: Specific discharge capacities of pouch cells (NMC 111 vs graphite) with unstructured and structured NMC cathodes (50 μm film thickness) for cycle numbers of 4000 cycles (1C/1C, unstructured NMC), 5000 cycles (2C/3C structured NMC) and 11,500 cycles (1C/1C structured NMC).

Pouch cells with structured NMC 111 cathodes with state-of-the-art film thickness show no spontaneous cell failure and could still provide more than 50 % of initial capacity even after 11,500 cycles. Figure 3 shows that at 1C / 1C and increased C-rates of 2C / 3C (charging/discharging) the 3D battery lifetime (80% of initial capacity) still exceeds 2000 cycles. Electrochemical cycling with 2C / 3C is typically for automotive stress test.

The 3D battery concept for ultra-thick film nickel-rich NMC cathode materials could be recently established. Electrodes with a thickness of up to 250 μm were realized for this purpose. Structuring using ultrafast laser ablation enables a high aspect ratio and defect free pattern down to the current collector (Figure 4 a). The active mass loss could be reduced to less than 5%. The periodicity of the line pattern is typically in the range of 200 μm to 600 μm [19]. NMC 622 cathodes were

assembled versus metallic lithium using the coin cell design. The impact of electrode thickness and laser structuring on the rate capability was investigated. Figure 4 b shows that for laser structured NMC 622 electrodes with a thickness of up to 210 μm , the discharge capacity could be maintained even for high power operation (C-rate of 2C, i.e., charging and discharging is each performed within 30 minutes). For cells with unstructured NMC 622 electrodes of same thickness the capacity drops dramatically even for low power operation. An increase in NMC film thickness from state-of-the-art 50 μm up to 210 μm corresponds to an increase in energy density of about 26 % according to [17]. Thus, it could be proven for the first time for this type of battery system that high energy density and high power operation are possible at once.

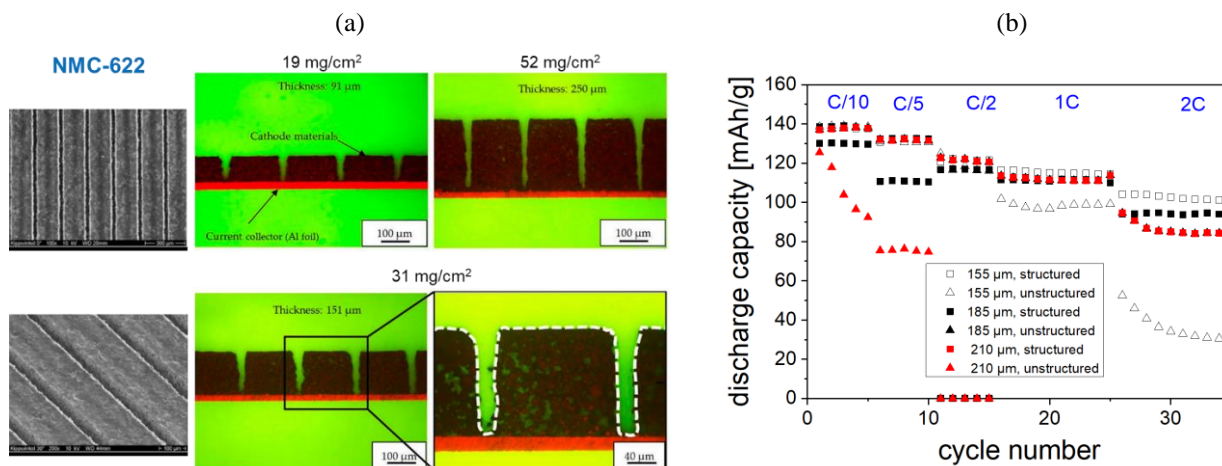


Figure 4: Laser structured $\text{Li}(\text{Ni}_{0.6}\text{Mn}_{0.2}\text{Co}_{0.2})\text{O}_2$ (NMC 622) cathodes and their impact on electrochemical performance: (a) SEM images of laser structured NMC 622 cathodes with 200 μm pitch distance (film thickness 91 μm) and cross-sectional view of NMC 622 cathodes with different film thicknesses (line distance 200 μm) [34]; (b) specific discharge capacity as a function of cycle number for lithium-ion cells with structured and unstructured NMC 111 thick-film electrodes for different discharge C-rates and electrode film thickness (155 μm , 185 μm , 210 μm) [19].

3.2 Anode

In recent studies the research was focused on graphite-based anodes because this electrode type is mainly responsible for fast charging issues and related lithium plating scenarios. Due to the preferred orientation of flake-like graphite particles and related diffusion planes, an anisotropy of lithium-ion diffusion kinetics is achieved. Thus, a small increase in electrode film thickness results in a disproportionate decrease in capacity with increasing C-rate. Figure 5 a shows such an impact, i.e., a significant drop in capacity at C-rates of 2C, while the film thickness was only slightly increased from 56 μm to 76 μm .

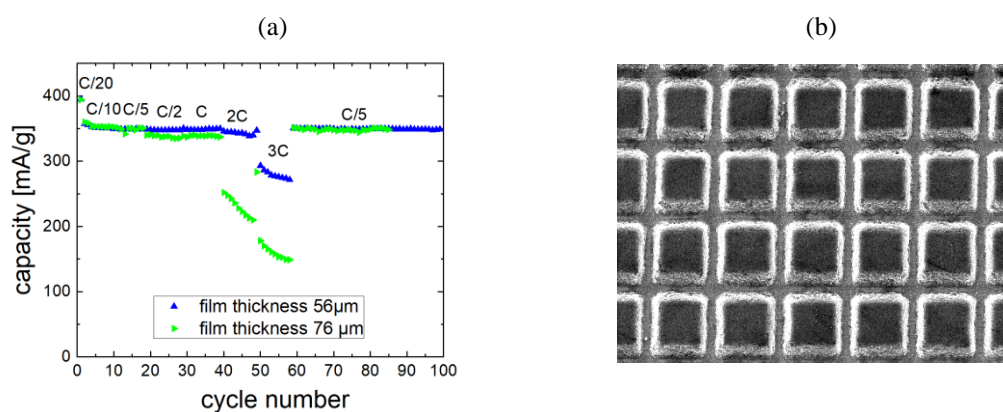


Figure 5: Laser structuring of anodes: (a) capacity of half-cells assembled with state-of-the-art thin film graphite anodes as function of cycle number for different C-rates; (b) laser structured silicon-graphite anode with grid design (periodicity 100 μm). However, the high capacity retention at C/5 for cycle numbers of 60 to 100 shows that the drop in capacity at 2C and 3C is not related to degradation processes but to a rise of cell polarisation and limited diffusion kinetics. Ultrafast laser structuring of graphite anodes as well as high energy silicon-graphite anodes (Figure 5 b) leads to an improved lithium-ion

diffusion kinetics caused by new lithium migration pathways provided by an increased active surface (not shown here, please refer to [25]). Cells with structured anodes of same film thickness provide a significant higher capacity in comparison to cells with unstructured electrodes. The capacity is quite stable for C rates up to 3C. These are incredible outstanding results proving the 3D battery concept also for the anode materials. The generated high aspect ratio channels can have a width smaller than 20 μm . No debris was formed onto the surface which would might be a problem during electrode stacking (Figure 5 b). Large particles on top of the electrodes would lead to a serious damage of the electrical insulating separator layers. Also no thermal impact or selective binder removal was detected. Grid patterns seem to be most appropriate for silicon graphite electrodes. With only 20 weight percentage of silicon in the anode one can almost double the specific capacity in comparison to the pure graphite anode. While for the unstructured silicon-graphite electrode the capacity drops quite fast with increasing C rate due to mechanical degradation, the capacity of the grid patterned silicon-graphite electrode maintains almost constant at high values, referring to [25].

Laser structuring of electrodes can reduce mechanical degradation but also can improve lithium-ion diffusion kinetics. For investigating lithium-ion diffusion pathways and the impact of 3D structuring, laser induced breakdown spectroscopy was performed on model graphite electrodes. The freestanding micro pillars have a footprint of 600 x 600 μm^2 . The film thickness is 100 μm . The lithium elemental mapping in cross section view shows that the laser generated side walls became activated at elevated C-rates by providing new lithium diffusion pathways. The diffusion lengths from the sidewall is almost one order of magnitude higher in comparison to the diffusion lengths from top of the electrode. The diffusion anisotropy in flake-like graphite anodes is significantly reduced by laser generated artificial porosity [30].

Post mortem studies applying LIBS was also performed at silicon-graphite anodes for which the mechanical degradation is significant higher than for pure graphite electrodes. In Figure 6 lithium distribution is illustrated in unstructured (Figure 6 a) and structured (Figure 6 b) silicon-graphite electrodes after lithiation of the electrode which corresponds to the scenario of fast charging of a lithium-ion battery.

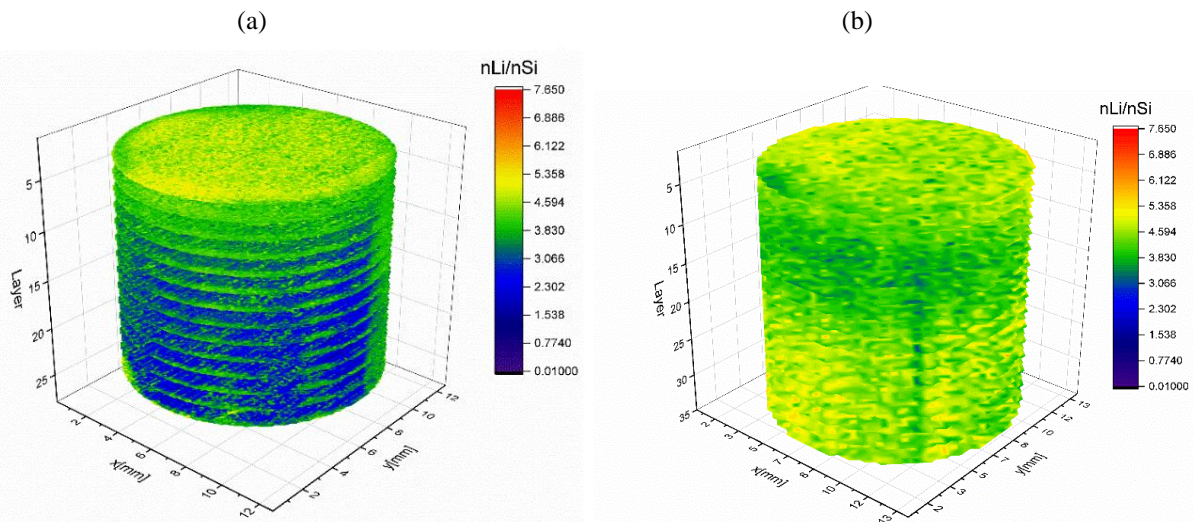


Figure 6: 3D lithium elemental mapping achieved by LIBS (post mortem) for (a) unstructured and (b) structured Si/C electrodes which were lithiated at 1C [26].

In case of using unstructured electrodes lithium is only embedded in the top layers of the electrode (Figure 6 a). That means only a small fraction of available capacity is used. In contrast to that is the charging of batteries, i.e., lithiation of anode, using structured silicon-graphite anodes. A homogeneous and almost saturated lithium distribution in the entire electrodes is achieved (Figure 6 b) silicon. These electrodes are good for fast charging operation.

Finally, it is worth mentioning that pouch cells with structured electrodes, cathodes and anodes, show the best electrochemical performance data such as an enhanced high rate capability and a significant increase in battery lifetime. It could be proven for next generation thick film electrodes that the battery lifetime - indicated by end of life measurements - can be almost doubled by applying the 3D battery concept. However, in dependence of material and application scenario a respective process development is required. For example, laser structuring of small channels can lead to V-shaped cross sections as function of process parameters. Thus, during lithiation the lower part off the electrode can become inactive [26]. High mechanical pressures avoids further lithiation even into the graphite particles. To overcome those bottlenecks

an adaption of structure design to the respective application becomes necessary. Appropriate laser parameters and processing strategies can be developed to realize rectangular channel geometries that are more suitable to preserve the reversible lithium accessibility of the entire electrode.

4. CONCLUSION

Structuring of anodes boosts the charging performance while structuring of cathodes is required to enable simultaneously high power and high energy battery operation. An enhanced battery lifetime is gained which was demonstrated for state-of-the-art and next generation battery materials. The 3D battery concept also significantly improves the electrolyte wetting of the battery materials which finally will lead to a remarkable reduction of scrap rate in battery production. In related research it could be also shown that a positive impact regarding a reduced lithium plating and therefore a benefit with regard to battery safety can be expected as well [39]. Besides an optimization of electrode architectures with regard to application scenario, the upscaling of the laser process with regard to the required integration in battery manufacturing is a challenging and rather important task in current research and development. A first approach during upscaling would be simply increasing the laser power and using ultrashort laser pulses. For thin films and medium size footprints this approach provide a rather good pattern and surface quality. However, the processing speed has further to be increased as well as the film thickness and electrode footprint for high energy applications. For next generation of thick film and large footprint batteries the laser structuring process therefore has to be further optimized with regard to its processing speed. This is currently performed in the industrial guided project called NextGen3DBat [21]. In the center of activity is the development of a suitable OEM laser radiation source with further increased average laser power while the laser pulse duration is kept in the ultrafast regime. This is quite important in order to realize a laser structuring process without any thermal impact to the sensitive active battery materials. The high power enables the use of a multi-beam laser ablation approach by using diffractive optical elements. In this approach the processing speed can be increased by a factor of 5. At KIT roll-to-roll infrastructures for laser processing of commercial and sophisticated electrodes with high precision and processing speed are enabling pilot line level. In current projects pouch cells with structured electrodes and a capacity up to 20 Ah are being built.

5. ACKNOWLEDGEMENTS

I am grateful for the help of my colleagues, A. Reif, A. Meyer, Y. Zheng, P. Zhu, H. Besser, P. Smyrek, and M. Kapitz for their technical support and assistance in laser processing, material characterization, and battery analyses. This research was funded by the Federal Ministry of Education and Research (BMBF), project NextGen-3DBat, project No. 03XP01798F.

6. REFERENCES

1. Dühnen, S., J. Betz, M. Kolek, R. Schmuch, M. Winter, and T. Placke, *Toward green battery cells: perspective on materials and technologies*. Small Methods, 2020. 4(7): p. 2000039.
2. Nykvist, B. and M. Nilsson, *Rapidly falling costs of battery packs for electric vehicles*. Nature climate change, 2015. 5(4): p. 329-332.
3. Wood III, D.L., J. Li, and C. Daniel, *Prospects for reducing the processing cost of lithium ion batteries*. Journal of Power Sources, 2015. 275: p. 234-242.
4. Mauler, L., F. Duffner, W.G. Zeier, and J. Leker, *Battery cost forecasting: a review of methods and results with an outlook to 2050*. Energy & Environmental Science, 2021. 14: p. 4712-4739.
5. Andre, D., S.-J. Kim, P. Lamp, S.F. Lux, F. Maglia, O. Paschos, and B. Stiaszny, *Future generations of cathode materials: an automotive industry perspective*. Journal of Materials Chemistry A, 2015. 3(13): p. 6709-6732.
6. Liu, J., Z. Bao, Y. Cui, E.J. Dufek, J.B. Goodenough, P. Khalifah, Q. Li, B.Y. Liaw, P. Liu, and A. Manthiram, *Pathways for practical high-energy long-cycling lithium metal batteries*. Nature Energy, 2019. 4(3): p. 180-186.
7. Bracklo, C., K. Bratz, and R. Echtermeyer, *Fortschrittsbericht 2018 – Markthochlaufphase*. 2018, Berlin: Nationale Plattform Elektromobilität (NPE).
8. Armand, M., P. Axmann, D. Bresser, M. Copley, K. Edström, C. Ekberg, D. Guyomard, B. Lestriez, P. Novák, and M. Petranikova, *Lithium-ion batteries—Current state of the art and anticipated developments*. Journal of Power Sources, 2020. 479: p. 228708.

9. Li, T., X.-Z. Yuan, L. Zhang, D. Song, K. Shi, and C. Bock, *Degradation mechanisms and mitigation strategies of nickel-rich NMC-based lithium-ion batteries*. *Electrochemical Energy Reviews*, 2020. 3(1): p. 43-80.
10. Niketic, S., C.-H. Yim, J. Zhou, J. Wang, and Y. Abu-Lebdeh, *Influence of Ti Substitution on Electrochemical Performance and Evolution of $\text{LiMn}_{1.5-x}\text{Ni}_{0.5}\text{Ti}_x\text{O}_4$ ($x=0.05, 0.1, 0.3$) as a High Voltage Cathode Material with a Very Long Cycle Life*. *Inorganics*, 2022. 10(1): p. 10.
11. Wood, D.L., J.D. Quass, J. Li, S. Ahmed, D. Ventola, and C. Daniel, *Technical and economic analysis of solvent-based lithium-ion electrode drying with water and NMP*. *Drying Technology*, 2018. 36(2): p. 234-244.
12. Azhari, L., X. Zhou, B. Sousa, Z. Yang, G. Gao, and Y. Wang, *Effects of Extended Aqueous Processing on Structure, Chemistry, and Performance of Polycrystalline $\text{LiNi}_x\text{Mn}_y\text{Co}_z\text{O}_2$ Cathode Powders*. *ACS Applied Materials & Interfaces*, 2020. 12(52): p. 57963-57974.
13. Wood, M., J. Li, R.E. Ruther, Z. Du, E.C. Self, H.M. Meyer III, C. Daniel, I. Belharouak, and D.L. Wood III, *Chemical stability and long-term cell performance of low-cobalt, Ni-Rich cathodes prepared by aqueous processing for high-energy Li-Ion batteries*. *Energy Storage Materials*, 2020. 24: p. 188-197.
14. Zhu, P., J. Han, and W. Pfleging, *Characterization and Laser Structuring of Aqueous Processed $\text{Li}(\text{Ni}_{0.6}\text{Mn}_{0.2}\text{Co}_{0.2})\text{O}_2$ Thick-Film Cathodes for Lithium-Ion Batteries*. *Nanomaterials*, 2021. 11(7): p. 1840.
15. Gotcu, P. and H. Buqa. *A reliable large-scale implementation of water-based slurry technology for production of high-performance lithium-ion batterie*. in *International Battery Production Conference*. 2020. Online: WiTech Engineering GmbH.
16. Neidhart, L., K. Fröhlich, N. Eshraghi, D. Cupid, F. Winter, and M. Jahn, *Aqueous Manufacturing of Defect-Free Thick Multi-Layer NMC811 Electrodes*. *Nanomaterials*, 2022. 12(3): p. 317.
17. Pfleging, W., *Recent progress in laser texturing of battery materials: a review of tuning electrochemical performances, related material development, and prospects for large-scale manufacturing*. *International Journal of Extreme Manufacturing*, 2021. 3: p. 012002 (20pp).
18. Ding, Y., Z.P. Cano, A. Yu, J. Lu, and Z. Chen, *Automotive Li-ion batteries: current status and future perspectives*. *Electrochemical Energy Reviews*, 2019. 2(1): p. 1-28.
19. Pfleging, W., *A review of laser electrode processing for development and manufacturing of lithium-ion batteries*. *Nanophotonics*, 2018. 7(3): p. 549-573.
20. Long, J.W., B. Dunn, D.R. Rolison, and H.S. White, *Three-dimensional battery architectures*. *Chemical Reviews*, 2004. 104(10): p. 4463-4492.
21. Meyer, A., Y. Sterzl, S. Xiao, U. Rädcl, and W. Pfleging, *Ablation behaviour of electrode materials during high power and high repetition rate laser structuring*. *Proc. of SPIE*, 2022. 11989: p. 119890G-1 (10pp).
22. Tarascon, J.M. and M. Armand, *Issues and challenges facing rechargeable lithium batteries*. *Nature*, 2001. 414(6861): p. 359-367.
23. Tariq, F., V. Yufit, D.S. Eastwood, Y. Merla, M. Biton, B. Wu, Z. Chen, K. Freedman, G. Offer, and E. Peled, *In-operando X-ray tomography study of lithiation induced delamination of Si based anodes for lithium-ion batteries*. *ECS Electrochemistry Letters*, 2014. 3(7): p. A76.
24. Obrovac, M.N. and L.J. Krause, *Reversible Cycling of Crystalline Silicon Powder*. *Journal of The Electrochemical Society*, 2007. 154(2): p. A103.
25. Zheng, Y., H. Seifert, H. Shi, Y. Zhang, C. Kübel, and W. Pfleging, *3D silicon/graphite composite electrodes for high-energy lithium-ion batteries*. *Electrochimica Acta*, 2019. 317: p. 502-508.
26. Zheng, Y., D. Yin, H.J. Seifert, and W. Pfleging, *Investigation of Fast-Charging and Degradation Processes in 3D Silicon-Graphite Anodes*. *Nanomaterials*, 2022. 12(1): p. 140.
27. Kwade, A., W. Haselrieder, R. Leithoff, A. Modlinger, F. Dietrich, and K. Droeder, *Current status and challenges for automotive battery production technologies*. *Nature Energy*, 2018. 3(4): p. 290-300.
28. Schmuck, R., R. Wagner, G. Hörpel, T. Placke, and M. Winter, *Performance and cost of materials for lithium-based rechargeable automotive batteries*. *Nature Energy*, 2018. 3(4): p. 267-278.
29. Pfleging, W., *Recent Progress in Laser Texturing of Battery Materials: A Review of Tuning Electrochemical Performances, Related Material Development, and Prospects for Large-Scale Manufacturing*. *International Journal of Extreme Manufacturing*, 2020. 3: p. 1.

30. Zheng, Y., L. Pfäffl, H.J. Seifert, and W. Pfleging, *Lithium distribution in structured graphite anodes investigated by laser-induced breakdown spectroscopy*. Applied Sciences, 2019. 9(20): p. 4218.
31. Smyrek, P., J. Pröll, H. Seifert, and W. Pfleging, *Laser-induced breakdown spectroscopy of laser-structured Li (NiMnCo) O₂ electrodes for lithium-ion batteries*. Journal of the Electrochemical Society, 2015. 163(2): p. A19.
32. Pfleging, W., Y. Zheng, M. Mangang, M. Bruns, and P. Smyrek, *Laser processes and analytics for high power 3D battery materials*. Proc. of SPIE, 2016. 9740: p. 974013 (9pp).
33. Smyrek, P., T. Bergfeldt, H.J. Seifert, and W. Pfleging, *Laser-induced breakdown spectroscopy for the quantitative measurement of lithium concentration profiles in structured and unstructured electrodes*. Journal of Materials Chemistry A, 2019. 7(10): p. 5656-5665.
34. Zhu, P., H.J. Seifert, and W. Pfleging, *The ultrafast laser ablation of Li (Ni_{0.6}Mn_{0.2}Co_{0.2})O₂ electrodes with high mass loading*. Applied Sciences, 2019. 9(19): p. 4067.
35. Song, Z., P. Zhu, W. Pfleging, and J. Sun, *Electrochemical performance of thick-film Li (Ni_{0.6}Mn_{0.2}Co_{0.2})O₂ cathode with hierarchic structures and laser ablation*. Nanomaterials, 2021. 11(11): p. 2962.
36. Meyer, A., F. Ball, and W. Pfleging, *The Effect of Silicon Grade and Electrode Architecture on the Performance of Advanced Anodes for Next Generation Lithium-Ion Cells*. Nanomaterials, 2021. 11(12): p. 3448.
37. Pfleging, W., P. Smyrek, J. Hund, T. Bergfeldt, and J. Pröll. *Surface micro-structuring of intercalation cathode materials for lithium-ion batteries: a study of laser-assisted cone formation*. in *Laser-based Micro-and Nanoprocessing IX*. 2015. International Society for Optics and Photonics.
38. Pfleging, W. and J. Pröll, *A new approach for rapid electrolyte wetting in tape cast electrodes for lithium-ion batteries*. Journal of Materials Chemistry A, 2014. 2(36): p. 14918-14926.
39. Habedank, J.B., J. Kriegler, and M.F. Zaeh, *Enhanced fast charging and reduced lithium-plating by laser-structured anodes for lithium-ion batteries*. Journal of The Electrochemical Society, 2019. 166(16): p. A3940.